Available online at www.sciencedirect.com
SCIENCE DIRECT®
Journal of Crystal Growth 275 (2005) e1029–e1033
JOURNAL OF CRYSTAL GROWTH
www.elsevier.com/locate/jcrysgro

Phase behaviour in supported mixed monolayers of alkanols, investigated by AFM

A.N. Zdravkova*, J.P.J.M. van der Eerden, M.M.E. Snel

Department of Condensed Matter and Interfaces, Debye Institute, Utrecht University, P.O. Box 80000, 3508 TA Utrecht, The Netherlands

Available online 8 December 2004

Abstract

The structure of mixed Langmuir–Blodgett monolayers of fatty alcohols, $C_nH_{2n+1}OH$ with even $n = 16$–24, was investigated by AFM at 20–22 °C. Phase separation was found for compressed films, if the chain length of the two components differed at least 6 carbon atoms. A strong dependence of the domain shape on the surface pressure was observed. The excess Gibbs energy ΔG^{ex} vs. surface pressure and mole fraction was calculated from π-A isotherms. In line with thermodynamic analysis, the tendency of phase separation increased with increasing ΔG^{ex}. A surprising and as yet unexplained result was that we sometimes observed clear phase separation already for $\Delta G^{ex} > -0.1RT$.

PACS: 64.75; 87.64.D; 68.55; 64.75; 68.18

Keywords: A1. Atomic force microscopy; A1. Langmuir–Blodgett technique; A1. Surface structure; A3. LB monolayer; B1. Fatty alcohols

1. Introduction

Aliphatic long-chain alcohols C_n ($C_nH_{2n+1}OH$ with $n = 16$–31) can be adsorbed on water surfaces. Interestingly, adsorbed C_n enhances ice nucleation. Grazing-incidence X-ray diffraction (GID) studies of C_n monolayers on water at 5 °C revealed two-dimensional structure formation. Wang et al. [1] concluded that the molecules in the C_n monolayers adopt a herringbone pattern. According to GID data, monolayers with $n = 16$ and 20 contain less crystalline material than monolayers with $n = 23$, 30, 31 [2]. IR spectra of the same alcohol monolayers at an area per molecule of 20 Å^2 have been measured at the air/water interface at 20 °C. These measurements also showed that the hydrocarbon chains become more ordered with increasing length. It was found that only alcohols with molecular areas of 18.5–20 Å^2 significantly enhance nucleation of ice [2].

*Corresponding author. Fax: +31 30 2532403.
E-mail address: a.n.zdravkova@chem.uu.nl
‘(A.N. Zdravkova).

0022-0248/$ - see front matter © 2004 Elsevier B.V. All rights reserved.
doi:10.1016/j.jcrysgro.2004.11.073

Combining these two types of experiments, we expect that 2D layers of long alcohols ($n > 20$) crystallize, when the molecular area is about 20 Å^2. Kulkarni et al. [3] investigated mixed monolayers of C_{16} and C_{22} at 25 °C, studying surface viscosity and the area per molecule. Isotherms of the system at five different mole fractions showed that all mixtures were thermodynamically non-ideal.

To better understand mixed monolayers and the effect of chain length on mixing, we investigated mixed monolayer films with AFM: C_{16}:C_{22} with stoichiometry 1:1, 1:3 and 3:1, C_{18}:C_{22} (1:1), C_{18}:C_{24} (1:1) and C_{16}:C_{24} (1:1). We used the Langmuir–Blodgett technique to transfer at several surface pressures binary mixed monolayers from the water/air interface onto a mica substrate. Equilibrium layers were obtained by using a very small initial surface pressure of the Langmuir layer, and compressing slowly to the final pressure.

2. Materials and methods

2.1. Chemicals

Film material: Fatty alcohols ($C_nH_{2n+1}OH$, with $n = 16, 18, 22, 24$) were obtained from Merck and used without further purification. Separate stock solutions of each alcohol with a concentration of 5 mM in distilled chloroform were prepared. Solutions containing 1 mM mixtures of the alcohols in mole ratios 1:1,1:3 and 3:1 were prepared by proper mixing and diluting of stock solutions.

Subphase: MiliQ water was used as the subphase in our Langmuir system for all experiments. The resistivity of the water is 18 MΩ cm.

Substrates: All monolayers were transferred onto freshly cleaved mica.

2.2. π-A isotherms

Compression isotherms were measured on a Teflon trough ($17.2 \times 35.7\,cm^2$). The spreading pressure π was measured with a Wilhelmy-type balance consisting of a platinum plate coupled to an electrobalance (Cahn Ankersmit, 2000), with an accuracy of about 0.1 mN/m. The film material was spread on the water subphase, using a 100 μL Hamilton syringe. The area per molecule A was controlled by a moving barrier, at an accuracy of 1–2 Å^2 per molecule. Spreading took place at $A \gg 100$ Å^2. Film compression started almost immediately after spreading, at a rate of 5 cm/min.

2.3. Langmuir–Blodgett film transfer

To obtain LB films, first a substrate was immersed perpendicularly in the aqueous subphase. Then the film material was spread on the water surface. Equilibrium layers were obtained by using a very small initial surface pressure ($\pi = 0$ mN/m) of the monolayer, and compressing slowly (1 cm/min) to the final pressure. Film transfer was then accomplished by vertically lifting the substrate through the air–water interface at a speed of 2 mm/min. After deposition the monolayers were dried in air and kept in close containers until use. All experiments were performed at 20–22 °C.

2.4. AFM measurements

The samples were examined with AFM within about 5 h after preparation. Imaging was done with a Nanoscope III (Digital Instruments) in contact mode with oxide-sharpened silicon nitride tip ($k = 0.06$ N/m). The AFM was equipped with an E-scanner.

3. AFM observations

3.1. C_{16}:C_{22}

The AFM images in Fig. 1 clearly show phase separation at surface pressures $\pi \geqslant 10$ mN/m. The thicker domains presumably mainly consist of C_{22}, the thinner mainly of C_{16}. The thickness of the C_{22} domains and of the surrounding C_{16} film was found to be less than the thickness calculated from X-ray data of crystals with vertically extended alcohols. The measured values are 1.0 nm (1.87 nm in crystals) for C_{16} and 2.0 nm (2.51 nm in crystals)

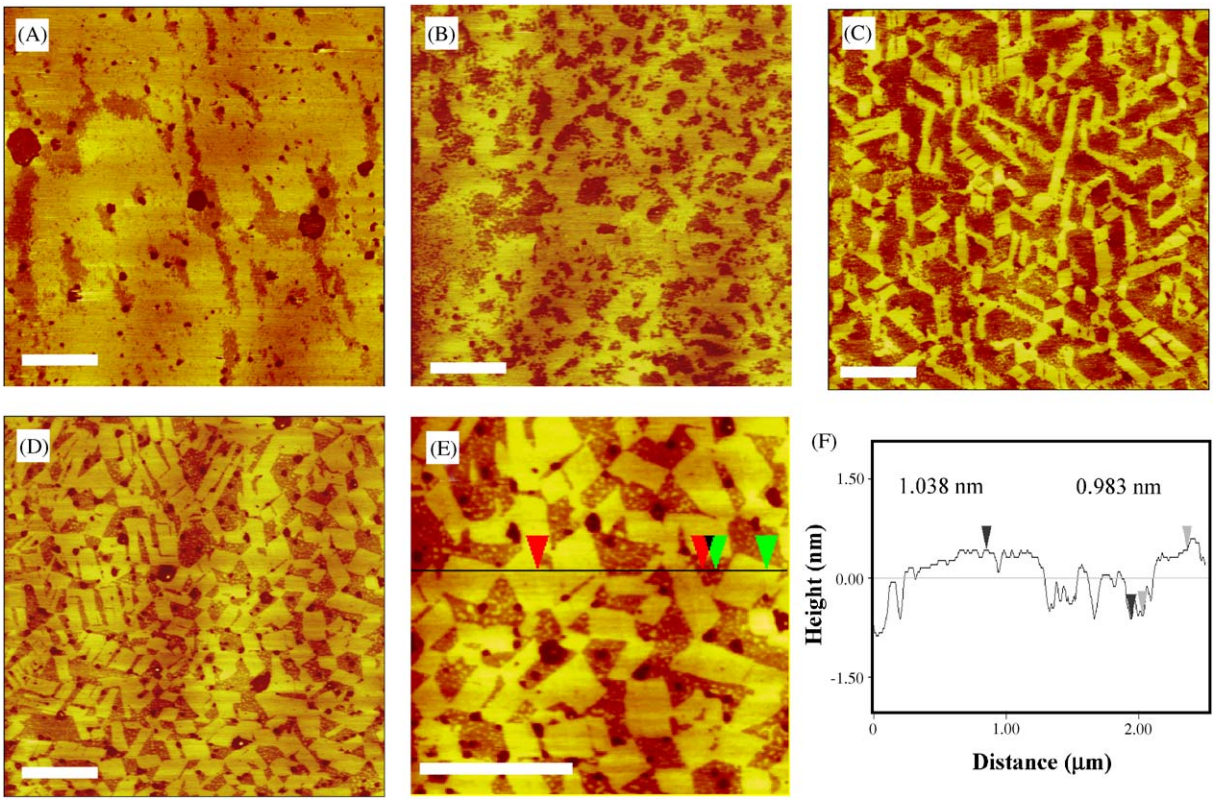

Fig. 1. AFM height image showing C_{16}:C_{22} (1:1) mixed monolayers transferred at surface pressure (A) $\pi = 10\,mN/m$, (B) $\pi = 15\,mN/m$, (C) $\pi = 20\,mN/m$ and (D) $\pi = 35\,mN/m$. In panel E, an enlarged height image is given, showing the tetragonal shape of C_{22} domains with corresponding cross section (F). The height difference between both alcohols is given by the vertical distance between the markers. The scale bar is 1 μm and the vertical scale is 4 nm for all images.

for C_{22}. This effect was observed before and explained as monolayer depression, caused by the AFM tip [4]. Fig. 1(F) shows the height difference between C16 and C22, to be 0.9–1.0 nm. Phase separation in domains with the same height difference was found for C16:C22 mixtures with (1:3) and (3:1) stoichiometry.

3.2. C_{18}:C_{22}

The AFM images of this system showed a homogeneous monolayer at all surface pressures at which the monolayer was compressed ($\pi = 10$, 20 and 35 mN/m). The measured thickness of the monolayer was ~2.1 nm at $\pi = 35\,mN/m$, as for C_{22} (images not shown).

3.3. C_{18}:C_{24}

This mixture with 6 carbon atoms length difference behaved similar to C_{16}:C_{22}. The AFM images showed phase separation with C_{24} domains embedded in C_{18}. At $\pi = 35\,mN/m$ the domains have tetragonal shapes and they are more ordered than in the C_{16}:C_{22} mixture (images not shown). The measured thickness for C_{18} is ~1.6 nm (2.09 nm in crystals) and for C_{24} it is 2.2–2.3 nm (2.7 nm in crystals).

3.4. C_{16}:C_{24}

We observed different C_{24} domain shapes as in other mixtures, they were very irregular, at all final

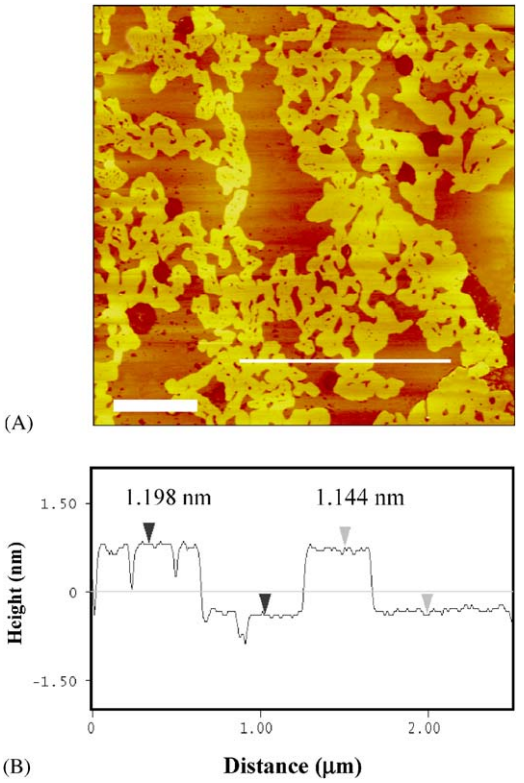

Fig. 2. AFM height image showing mixed monolayer of C_{16}:C_{24}, transferred at surface pressure $\pi = 35\,\mathrm{mN/m}$ (A) with the corresponding cross section (B). The scale bar is 1 μm. The vertical scale is 4 nm.

surface pressures. The height difference between the C_{24} domains and the C_{16} film is 1.1–1.2 nm (Fig. 2).

4. Thermodynamic analysis

At given spreading pressure π and average composition x the structure with the lowest possible Gibbs energy G (in J/mol) will be formed. Let G^{hom} be the Gibbs energy for a homogenous, uniform film. If $G^{\mathrm{hom}}(x,\pi)$ is a concave function of x, then a homogeneous film is thermodynamically stable and $G = G^{\mathrm{hom}}$. If $G^{\mathrm{hom}}(x,\pi)$ has a convex part, then a homogeneous film is unstable for a composition interval $x \in (x_0, x_1)$ that includes the convex part. A homogeneous film with $x \in (x_0, x_1)$ can decrease its Gibbs energy by phase separating in fractions $\tilde{x} = (x - x_0)/(x_1 - x_0)$ and $1 - \tilde{x} = (x_1 - x)/(x_1 - x_0)$ with composition x_1 and x_0, respectively:

$$x \in (x_0, x_1) \rightarrow G(x,\pi) = (1-\tilde{x})G(x_0,\pi) + \tilde{x}G(x_1,\pi) < G^{\mathrm{hom}}(x,\pi). \quad (1)$$

The points $x_0 = x_0(\pi)$ and $x_1 = x_1(\pi)$ are the common tangent points to G^{hom}. The molar Gibbs energy can be determined, using $(\partial G/\partial\pi)_x = A$ from $\pi - A$ diagrams

$$G(\pi) - G(\pi_\infty) = \int_{\pi_\infty}^{\pi} A(\pi')\,\mathrm{d}\pi' \approx \pi A(\pi) - RT - \int_{A(\pi)}^{\infty} \pi(A)\,\mathrm{d}A, \quad (2)$$

where π_∞ is the reference spreading pressure, which is chosen small enough that the film is thermodynamically ideal at π_∞. The Gibbs energy is split into an ideal and an excess part:

$$G(\pi,x) = G^{\mathrm{id}}(\pi,x) + G^{\mathrm{ex}}(\pi,x), \quad (3)$$

$$\frac{G^{\mathrm{id}}(\pi,x)}{RT} = (1-x)\frac{G_0(\pi)}{RT} + x\,\frac{G_1(\pi)}{RT} - x\,\ln(x) - (1-x)\ln(1-x). \quad (4)$$

The Gibbs energy of mixing is defined as

$$G^{\mathrm{mix}}(\pi,x) = G(\pi,x) - (1-x)G_0(\pi) - xG_1(\pi). \quad (5)$$

Since $G^{\mathrm{ex}}(\pi_\infty) = 0$, we get $G^{\mathrm{ex}}(x,\pi)$ of a mixture using the right-hand side of Eq. (2) for the mixed and pure films and substituting in Eq. (5). By definition a mixture is non-ideal if $G^{\mathrm{ex}}(x,\pi) \neq 0$. Using Eqs. (3)–(5) it is obvious that for ideal mixtures the so-called *additivity rule*

$$A(\pi,x) = (1-x)A_0(\pi) + xA_1(\pi) \quad (6)$$

holds [5]. Indeed, Eq. (6) holds for *completely* immiscible films as well. It is often believed that $G^{\mathrm{ex}}(x,\pi) > 0$ is necessary for phase separation to occur. In the most common case where phase separation is driven by energetically unfavourable mixing, i.e. $G^{\mathrm{hom,ex}} \geqslant 0$ for all x, $G^{\mathrm{ex}}(x,\pi) > 0$ indeed. However, phase separation may occur also if energetical or entropical reasons favour incorporation of a small fraction of the other component in a pure phase. Then $G^{\mathrm{hom,ex}}$ may have negative minima near x_0 and x_1, and a

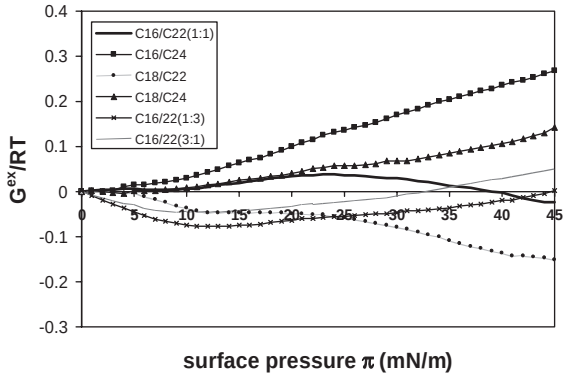

Fig. 3. Excess Gibbs energy for mixed monolayers as a function of spreading pressure π. The compositions of the mixture are given by the labels at the curves.

maximum in between. This can cause phase separation with $G^{ex}(x,\pi)<0$.

From this discussion it is clear that we need to measure $G^{ex}(x,\pi)$ accurately. At the low reference pressure π_0 the mixed film is ideal. We assume that upon decreasing the film area, it stays ideal down to the molar area $A=A^*(x)$ where π starts to increase. From Fig. 3 we see that, as in [3], $G^{ex}(x,\pi)$ is small as compared to RT for all mixtures, and that the noise is relatively large. Therefore the sign of $G^{ex}(x,\pi)$ cannot be determined unambiguously for C_{16}:C_{22} mixtures. The observed phase separation with AFM suggests a special interaction between the relatively flexible hydrophobic tails C_{16} and C_{22} alcohols, favouring incorporation of a small amount of C_{16} in C_{22} and reverse. The $G^{ex}(x=0.5,\pi)$ curve for the C_{16}:C_{22} mixture is similar to that for C_{18}:C_{24}, suggesting that the difference in chain length is the main parameter for demixing trends. Therefore $G^{ex}(x=0.5,\pi)$ tends to be negative for C_{18}:C_{22}, which favours homogeneous films and positive for C_{16}:C_{24}, which favours phase separation.

5. Conclusions

In this study we have obtained AFM images that reveal the structure of mixed alkanol monolayers, and we applied a thermodynamic analysis to interpret our observations.

The longer alcohols (C_{22} and C_{24}) interact more strongly, hence in a condensed layer they adopt a crystalline, herringbone crystal structure [1–2,6], unlike the shorter ones (C_{16} and C_{18}), which can be fluid like. This is in agreement with IR spectra for single alcohol monolayers at 20 °C [2].

For surface pressures of $\pi=10$–35 mN/m we found phase separation for all systems, except for C_{18}:C_{22}, with domains of the longer alcohol, embedded in a shorter alcohol film. This suggests that in a condensed monolayer phase separation takes place when the chain length difference is at least 6 carbon atoms.

At high surface pressure, $\pi=20$–35 mN/m, the domains are tetragonal shaped. This can be understood as at higher pressures crystalline packing of molecules is favoured. The π-A isotherms show an area per molecule 19–20 Å^2 for these surface pressures. At lower pressures, $\pi=10$–15 mN/m, the excess Gibbs energy is small. Then disordered packing is more favourable and domains are rounded.

If the chain length difference is only 4 carbon atoms, both the AFM images and the thermodynamic data of the C_{18}:C_{22} mixture indicate no phase separation.

For a chain length difference of 8 units the excess Gibbs energy is so large that the driving force for phase separation might be beyond the limit where equilibrium structures are formed. Hence we speculate that the irregular domain shapes in the C_{16}:C_{24} mixture are growth shapes, rather than thermodynamic equilibrium shapes.

The surprising result that we observed, phase separation already in the range where our thermodynamic measurements indicated $\Delta G^{ex}\cong 0.1RT$, cannot be explained yet, but it might be due to a too-high compression rate around the spreading pressure where phase separation starts.

References

[1] J.L. Wang, et al., J. Am. Chem. Soc. 116 (1994) 1192.
[2] R. Popovitz-Biro, et al., J. Am. Chem. Soc. 116 (1994) 1179.
[3] V.S. Kulkarni, et al., J. Colloid Interface Sci. 89 (1982) 40.
[4] E. ten Grotenhuis, et al., Colloids Surf. A 105 (1995) 309.
[5] G.L. Gains Jr., Insoluble Monolayers at Liquid–Gas Interfaces, Interscience, New York, 1966.
[6] M. Gavish, et al., Science 250 (1990) 973.